Brush Plated Copper Gallium Sulphide Films and their Properties

B. Kajamaideen[1], A. Panneerselvam[2] and K. R. Murali [3,]*

[1] Department of Science and humanities (Physics), KIT-Kalaignarkarunanidhi Institute of Technology, Coimbatore 641 402, India.
[2] Department of Physics, Paavai Engineering College, Paachal, India
[3] ECMS Division, CSIR-CECRI, Karaikudi -630 006, India.

Abstract: Copper gallium sulphide films were deposited for the first time by the brush plating technique at different electrolyte temperatures in the range of 30°C - 80°C and at a constant deposition current density of 5.0 mA cm-2. X-ray diffractograms of the films are single phase with chalcopyrite structure. EDAX measurements indicated that the Cu/Ga ratio decreased from 1.29 to 1.00 as the electrolyte temperature increased from 30°C - 80°C. The grain size increased with increase of electrolyte temperature. The grain size increases from 100 nm to 300 nm as the electrolyte temperature increases.

Keywords: brush elctrodeposition technique, thin film, semiconductor, electronic material, chalcopyrite

1 Introduction

Polycrystalline $CuGaS_2$, a ternary compound that has relatively low toxicity, has a direct optical band gap of about 2.4 eV - 2.5 eV. For this reason, the $CuGaS_2$ has been expected to be adopted as a Cd-free window layer for $Cu(In_{1-x}Ga_x)Se_2$-type solar cell or a green light-emitting material (Birkmire 2001, Jager-Waldau 2004) $CuGaS_2$ thin films can be prepared through various methods such as Modulated Flux Deposition (MFD) (Guillen & Herrero 2006), Metal-Organic Vapour-Phase Epitaxy (MOVPE) (Branch et al 2005), Electron Beam Evaporation (Jeong & Park 2003) and Metal-Organic Chemical Vapour Deposition (MOCVD) (Chichibu et al 1995). In this work, the brush electrodeposition technique has been employed for the first time to deposit $CuGaS_2$ films.

In this work, the brush electrode position technique was employed, to deposit $CuInS_2$ films for the first time. Brush plating technique is an electroplating process performed with hand held portable tool rather than a tank of solution is known as brush plating. The brush plating processes are also called as contact plating, selective plating or swab platting. This is essentially a plating method, deposition of a metal on the surface by electrochemical means, where the work is connected cathodically to the current source. The plating is then applied by means of a brush or swab, soaked with solution and connected to a flexible anode cable. A direct current power pack drives the electrochemical

reaction, depositing the desired metal on the surface of the substrate.

In practice, movement between the anode and cathode is required for optimum results when plating, stripping, activating and so on. Currently a broad range of metals can be plated by brush plating. The key advantage of selective plating is portability. Many systems can be moved to various locations in a production facility or be transported to the job site. Selective plating is also versatile since it permits most electroplate types to be deposited onto any conductive substrate that can be touched with an electrode. Selective plating allows higher current densities than tank plating, which translates into higher deposition rates, up to 0.01 mm min^{-1}. In addition, inherently precise thickness control permits plate buildup or repair without the need for subsequent machining. Controlling continuous movement between the anode and the work piece or cathode, is a key element in obtaining high quality brush plated deposits. However, quality also depends on plating within a specific current density range. The visual appearance of electroplate is also an indicator of quality. A dark grey or black deposit usually corresponds to a burnt deposit, which results from too high current densities or insufficient movement. In contrast, inadequate current density or too much movement produces a generally shiny surface. The films were

---

*Corresponding author E-mail: muraliramkrish@gmail.com

characterized by X-ray diffraction for structural analysis using Philips X-ray diffractometer with Cu Ka radiation (k = 1:5,418 A °). Hitachi U 3400 UV–VIS–NIR spectrophotometer was used to carryout the optical studies. Morphological studies were madewith JOEL 35 CFM scanning electron microscope.

2 Experimental Methods

Brush plating was carried out using Selectron Power Pack model 150 A - 40 V. Layers were brush plated on tin oxide coated conducting substrates of about 5.0 cm^2 which is the negative electrode. The stylus consisting of a carbon rod wrapped in cotton wool served as the anode. The cotton wool was held in position by a porous sleeve. Prior to plating, the stylus was wired to the power supply and the cotton wool was soaked in the electrolyte. The stylus was then brought into contact with the tin oxide substrate and moved at uniform speed. An electrical current was found passing whenever the stylus was in contact with the substrate. This is associated with the acceleration of the ions in the electrolyte trapped within the cotton wool which were subsequently reduced at the substrate to form the $CuGaS_2$ layer. The bath contained 5.0 mM of $GaCl_3$, 2.0 mM of $CuCl_2$ and 1.0 mM of sodium seleno sulphate at a pH of 1.5 was maintained throughout the experiment. In each case, the power unit was preset at a current density of 5.0 mA cm^{-2}. The electrolyte temperature was varied from 30°C - 80°C. The total deposition time was 20 min. Tin oxide coated glass and molybdenum sheets (0.1 mm thick) were used as substrates. Thickness of the $CuGaS_2$ films measured by Mitutoyo surface profilometer varied from 1.50 μm - 2.40 μm with increase of electrolyte temperature.
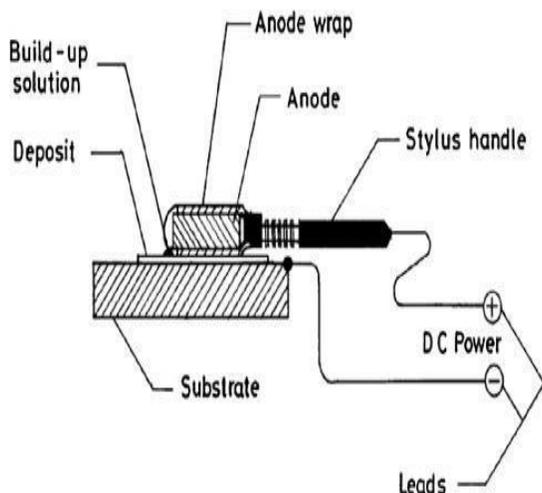

Fig. 1 Schematic of the brush plating system

3 Results and discussion

Figure.2 shows the x-ray diffraction patterns of $CuGaS_2$ films deposited at different electrolyte temperature. Peaks corresponding to (112), (204/220), (116/312) planes were observed in all the cases. As the electrolyte temperature

increased, the intensity of the peaks also increased. The XRD patterns were in good agreement with that of the tetragonal $CuGaS_2$ (JCPDS 25-0279). It is quite interesting to note that other phases such as $CuGa_3S_5$, $CuGa_5S_8$, Ga_2S_3, Cu_2S, and CuS (Branch et al 2005, Jeong & Park 2003) were absent. The evaluated lattice parameters are shown in Table.1
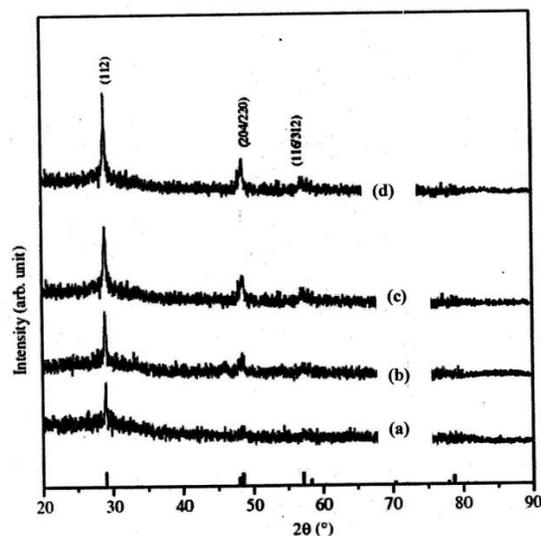

Fig. 2 X-ray diffraction pattern of $CuGaS_2$ films deposited at different electrolyte temperature (a) 30°C (b) 50°C (c) 70°C (d) 80°C.

The grain size of the films was calculated from the full width at half maximum of the diffraction profiles using Scherrer's Equation as shown in Equation (1) (Patterson 1939).

$$D = 0.95 \lambda / (\beta cos\theta) \tag{1}$$

where, D is the crystallite sixe, λ is the wavelength of CuKα radiation, β is the full width at half maximum, θ is the Bragg's angle. The crystallite size increased from 30 nm - 70 nm with increase of duty cycle. The crystallite size and thickness of the films are shown in Table 1. The dislocation density (*δ*) defined as the length of dislocation lines per unit volume of the crystal has been evaluated using the formula (Williamson & Smallman 1956).

$$\delta = 1/D^2 \tag{2}$$

Table 1 Microstructural parameters of $CuGaS_2$ films deposited at different electrolyte temperature

Electrolyte Temperature (°C)	Thickness (μm)	Lattice parameter (Å)		Grain size (nm)	Strain (x 10^{-4})	Dislocation density (x $10^{14}cm^{-3}$)
		"a"	"c"			

30	1.5	5.34	10.51	100	1.42	1.00
50	1.8	5.35	10.52	140	1.26	0.51
70	2.1	5.36	10.53	230	1.12	0.19
80	2.5	5.37	10.54	300	1.02	0.11

	Cu	Ga	S			
30	27.35	21.15	51.50	1.29	0.29	0.13
50	26.08	22.50	51.42	1.16	0.16	0.10
70	25.40	24.20	50.40	1.05	0.05	0.029
80	24.95	24.93	50.12	1.00	0.00	0.005

From the Table.2, it is observed that all the films are observed to contain excess sulphur. This is justified, since the deposition potential of sulphur is noble than that of copper and gallium and hence more sulphur will be deposited compared to copper or gallium.
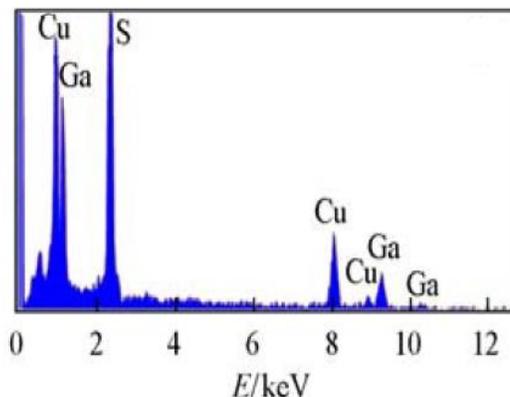
From the table, it is observed that the dislocation density decreases with increase of grain size. Information on the particle size and strain for the $CuGaS_2$ films was obtained from the full-width at half-maximum of the diffraction peaks. The full-width at half-maximum (β) can be expressed as a linear combination of the contributions from the particle size (D) and strain (ε) through the relation (Williamson & Hall 1953).

$$\beta cos\theta/\lambda = 1/D + \varepsilon\, sin\theta/\lambda \qquad (3)$$

The plot of $\beta cos\theta/\lambda$ vs $sin\theta/\lambda$ allows us to determine strain from slope of the   graph. The estimated values for films deposited at different electrolyte temperature are listed in Table 5.1. The deviation in the lattice parameter values from the bulk value observed in the present case clearly suggests that the grains in the films are under stress.

Such behaviour can be attributed to the change of nature, deposition conditions and the concentration of the native imperfections developed in thin films. This results in either elongation or compression of the lattice and the structural parameters. The density of the film is therefore found to change considerably in accordance with the variations observed with the lattice constant values (Sherif et al 1996).

The stress developed at higher duty cycles is likely due to the formation of native defects developed from the lattice misfit or dislocations. The defects have a probability to migrate parallel to the substrate surface with the surface mobility greatly influenced by the electrolyte temperature so that, the films will have a tendency to expand and develop an internal tensile stress. This type of change in internal stress is always predominant by the observed recrystallization process in polycrystalline films. The stress relaxation is mainly considered due to dislocation glides formed in the films. The decrease of internal stress may be attributed to a decrease in dislocation density. The reduction in the strain and dislocation density with increase of duty cycle may be due to the reduction in concentration of lattice imperfections due to the improved crystallinity at higher electrolyte temperature.

Table 2 Composition of $CuGaS_2$ films deposited at different electrolyte temperature

Electrolyte Temperature (°C)	Atomic Percentage (%)	Cu/Ga	Δm	Δs

Fig. 3   EDS spectrum of $CuGaS_2$ films deposited at 80°C electrolyte temperature

Composition of the films was determined from EDAX measurement (Figure 3). As the electrolyte temperature increased the films became more stoichiometric. Table.2 shows the composition of the films with electrolyte temperature. At lower electrolyte temperature, slight excess of copper is deposited compared to gallium. Since, the deposition potential for copper is more positive compared to indium and lower concentrations of gallium ions are available for deposition. At higher electrolyte temperature, the concentration of the gallium ion increases and the amount of gallium deposited increases, compared to that at lower electrolyte temperature. Due to the increase of gallium concentration, the Cu/Ga ratio approaches unity at electrolyte temperature. Based on the defect chemistry model of ternary compounds (Groenink & Janse 1978), these deviations from the stoichiometric composition can be described by two parameters Δm and Δs, which determine the deviations from the molecularity and stoichiometry respectively.

$$\Delta m = (Cu/Ga) - 1 \qquad (3)$$

$$\Delta s = \{2[S]/([Cu] + 3[Ga])\} - 1 \qquad (5)$$

The meanings of deviations from zero for these parameters are as follows

1.   Δm > 0 (Cu rich films); Δm < 0 (Ga rich films)

2. $\Delta s > 0$ (excess of sulphur); $\Delta s < 0$ (sulphur deficiency)

XPS studies were made on the $CuGaS_2$ films using MK II VG XPS system. From the Cu-2p core-level spectral region (Figure 4), the observed binding energy values for Cu-$2p_{3/2}$ (932.2 eV) and Cu-$2p_{1/2}$ (952.1 eV) are close to the reported values for Cu^+ (Cao & Shen 2011, Tang et al 2006).

Besides, the Cu-$2p_{2/3}$ satellite peaks characterizing Cu^{2+}, which are usually centered at about 942 eV (Xu et al 2011) are absent in the Figure 4. The Ga-2p core-level spectral region indicates that the binding energies for Ga-$2p_{3/2}$ (1118.02 eV) and Ga-$2p_{1/2}$ (1144.69 eV) are in good agreement with the respective values for Ga^{3+}. The S-2p core-level spectrum shows a peak located at 162.04 eV, which is also in agreement with the literature (Han et al 2006).
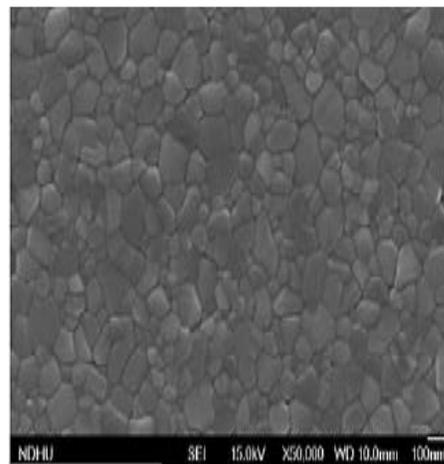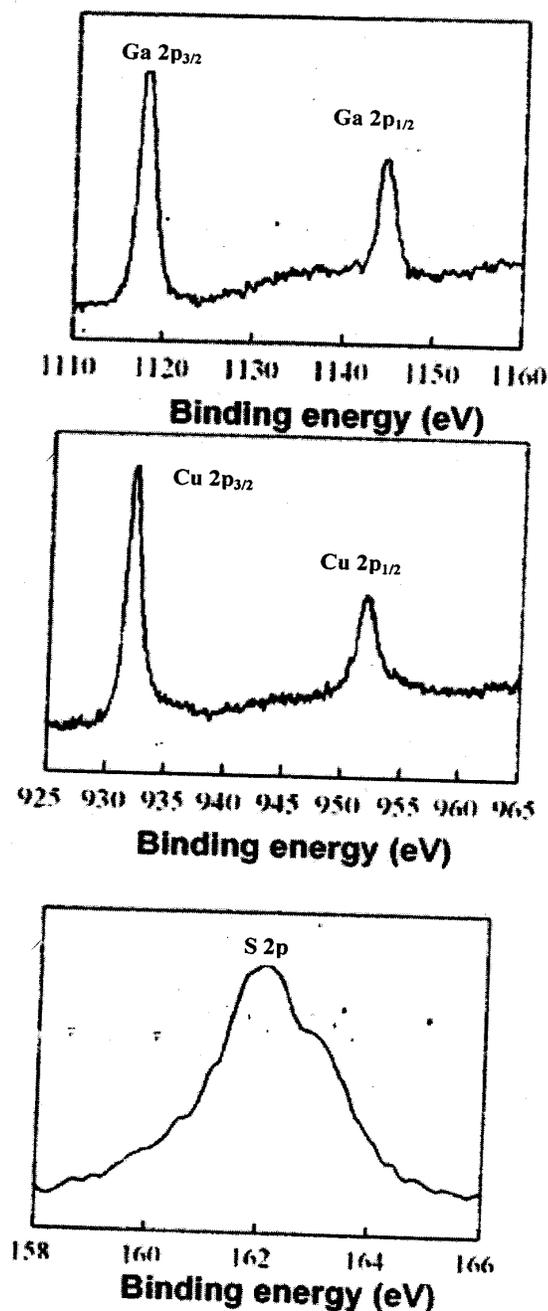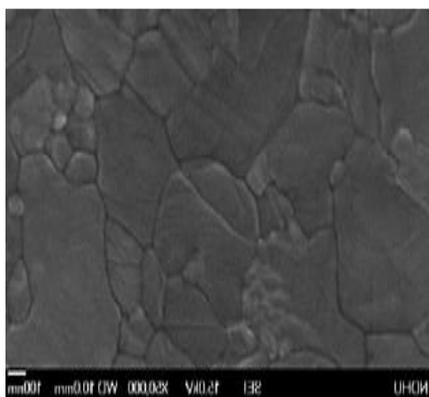

(a)
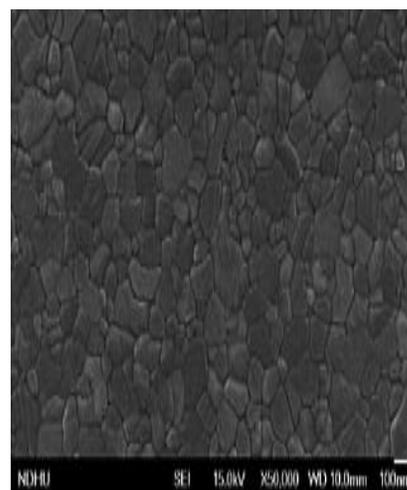
(b)

Fig. 4 XPS spectra of $CuGaS_2$ films deposited at 80°C electrolyte temperature.

(c)

Fig. 5   Scanning electron micrographs of CuGaS$_2$ films deposited at different electrolyte temperature (a) 30°C (b) 50°C (c) 80°C

Figure.5 shows the SEM micrographs for all the CuInS$_2$ films deposited with different electrolyte temperature. The surfaces are smooth and homogeneous with grain size around 100nm for electrolyte temperature of 30°C. The grain size further increased to 300nm for an electrolyte temperature of 80°C. At this temperature sufficient energy is available for particles to consolidate and to grow homogeneously in all direction. As result, higher electrolyte temperature grown films are composed of denser grains with smoother surface than the low temperature ones.

4 Conclusions

CuGaS$_2$ films have been deposited by the brush plating technique at different electrolyte temperature. The grain size is increased from 100 nm to 300 nm as the electrolyte temperature increases. X-ray diffractograms of the films indicate single phase chalcopyrite structure. EDAX measurements indicated that the Cu/Ga ratio decreased from 1.29 to 1.00 as the electrolyte temperature increased from 30°C - 80°C. Composition of the films was determined from EDAX measurement and stoichiometric composition can be described by molecularity and stoichiometry parameters. XPS spectrum exhibit the binding energies of Cu - 2p, Ga- 2p and S-2p peaks at 80°C electrolyte temperature.

References

[1] Birkmire, RW 2001, 'Compound polycrystalline solar cells:: Recent progress and Y2K perspective', Sol. Energy Mater. Sol. Cells, vol. 65, no. 1, pp. 17-28.

[2] Guillen, C & Herrero, J 2006, 'CuInS$_2$ and CuGaS$_2$ thin films grown by modulated flux deposition with various Cu contents', Phys. Status Solidi (A), vol. 203, no. 10, pp. 2438-2443.

[3] Jeong, WJ & Park, GC 2003, 'Structural and electrical properties of CuGaS$_2$ thin films by electron beam evaporation', Sol. Energy Mater. Sol. Cells, vol. 75, no. 1-2, pp. 93-100.

[4] Chichibu, S, Shirakata, S, Uchida, M, Harada, Y, Wakiyama, T, Matsumoto, S, Higuchi, H & Isomura, S 1995, 'Heteroepitaxial Growth of CuGaS$_2$ Layers by Low-Pressure Metalorganic Chemical Vapor Deposition', Jpn. J. Appl. Phys., vol. 34, Part 1, no. 8A, pp. 3991-3997.

[5] Branch, MS, Berndt, PR, Leitch, AWR, Botha, JR & Weber, J 2005, 'Structural and optical characterisation of CuGaS$_2$ thin films grown by MOVPE', Thin Solid Films, vol. 480-481, pp. 188-194.

[6] Patterson, AL 1939, 'The Scherrer formula for X-ray particle size determination', Phys. Rev, vol. 56, no. 10, pp. 978-982.

[7] Williamson, GK & Smallman, RE 1956, 'III. Dislocation densities in some annealed and cold-worked metals from measurements on the X-ray debye-scherrer spectrum', Phil. Mag., vol. 1, no. 1, pp. 34-46.

[8] Williamson, GK & Hall, WH 1953, 'X-ray Line Broadening from jiled Aluminium and Wolfram', Acta Metallurgica, vol. 1, no. 1, pp. 22-31.

[9] Groenink, JA & Janse, PH 1978, 'A generalized approach to the defect chemistry of ternary compounds', Z. Phys. Chem., vol. 110, no. 1, pp. 17-28.

[10] Han, K, Xiang, Z, Wang, Z, Wang, CL, Li, MJ, Zhang, JH & Yang, B 2006, 'A simple approach to fabricate CdS-SiO$_2$ hybrid microspheres by producing CdS nanoparticles on the surface of thiolated SiO$_2$ microspheres' , Chem. Res. Chinese Universities, vol. 22, no. 1, pp. 76-79.

[11] Soliman, LI & Ibrahim, AM 1997, 'Determination of optical constant of thermally evaporated CdSxSe1-x thin films using only transmission spectra', FIZIKA A, vol. 6, no. 4, pp. 181-189